Friction **9**(6): 1673–1687 (2021)
https://doi.org/10.1007/s40544-020-0460-6
ISSN 2223-7690
CN 10-1237/TH
RESEARCH ARTICLE

Exploring the role of $-NH_2$ functional groups of ethylenediamine in chemical mechanical polishing of GCr15 bearing steel

Hanqiang WU[1], Liang JIANG[1,*], Xia ZHONG[1], Jinwei LIU[1], Na QIN[2], Linmao QIAN[1]

[1] *Tribology Research Institute, State Key Laboratory of Traction Power, Southwest Jiaotong University, Chengdu 610031, China*

[2] *School of Mechanical Engineering, Southwest Jiaotong University, Chengdu 610031, China*

Received: 25 May 2020 / Revised: 06 August 2020 / Accepted: 01 October 2020

Abstract: Ethylenediamine with two $-NH_2$ functional groups was used as a critical complexing agent in chemical mechanical polishing (CMP) slurries for a high carbon chromium GCr15 bearing steel (equivalent to AISI 52100). The polishing performance and corresponding mechanism of $-NH_2$ functional groups were thoroughly investigated as a function of pH. It is revealed that, when polished with ethylenediamine and H_2O_2-based slurries, the material removal rate (MRR) and surface roughness R_a of GCr15 steel gradually decrease as pH increases. Compared with acidic pH of 4.0, at alkaline pH of 10.0, the surface film of GCr15 steel has much higher corrosion resistance and wear resistance, and thus the material removal caused by the pure corrosion and corrosion-enhanced wear are greatly inhibited, resulting in much lower MRR and R_a. Moreover, it is confirmed that a more protective composite film, consisting of more Fe^{3+} hydroxides/oxyhydroxides and complex compounds with $-NH_2$ functional groups of ethylenediamine, can be formed at pH of 10.0. Additionally, the polishing performance of pure iron and a medium carbon 45 steel exhibits a similar trend as GCr15 steel. The findings suggest that acidic pH could be feasible for amine groups-based complexing agents to achieve efficient CMP of iron-based metals.

Keywords: chemical mechanical polishing (CMP); complexing agent; bearing steel

1 Introduction

Bearing steels, such as a high carbon chromium GCr15 bearing steel (also named AISI 52,100, 100Cr6 and SUJ2. The chemical composition as follows: 0.95–1.05 wt% C, 1.30–1.65 wt% Cr, 0.15–0.35 wt% Si, 0.2–0.4 wt% Mn, < 0.027 wt% P, < 0.02 wt% S, and balance Fe [1]), have been widely used in industrial key basic parts such as bearings due to their superior properties [2]. It was found that, under the harsh working conditions, smooth surfaces of the contact elements of bearings can result in a decrease in the heat generation rate and a significant improvement of the lubrication performance between the rollers and the raceways [3, 4]. Moreover, the decrease in the surface roughness of the contact elements can improve the ratio between the thickness of the lubricating film and the composite roughness, which can effectively extend the service life of bearings [5]. Therefore, ultra-smooth surfaces are required to improve the service life and operation performance of ultra-precise devices which rely on bearings and other key basic parts made of bearing steels. However, traditional machining techniques, such as grinding and lapping, might not be able to meet such

* Corresponding author: Liang JIANG, E-mail: jiangliang@swjtu.edu.cn

stringent requirements [6]. Therefore, it is urgent to develop an efficient ultra-precision machining technique to achieve an ultra-smooth surface.

Chemical mechanical polishing (CMP) technique has been intensively used in the semiconductor industry for manufacturing ultra-large scale integrated circuits [7–9]. CMP can achieve an ultra-smooth and damage-free surface by the synergistic effect of chemical and mechanical interactions [7, 8]. For this reason, CMP has been gradually applied in processing key basic parts with bearing steels as the main material, such as GCr15 steel [10–14]. The complexing agent is one of the most critical additives for metals CMP, and it is used to enhance the material removal rate (MRR) as well as to reduce defects by chelating metal ions to form soluble complexes. Complexing agents containing $–NH_2$ functional groups are widely used in H_2O_2-based slurries for CMP of metals, such as copper [15–17]. Liu et al. [15] reported that the copper MRR increased with the concentration of ethylenediamine (containing two $–NH_2$ functional groups) increasing, and a rather high copper MRR of 1,899 nm/min could be achieved with the slurry containing 0.1 M ethylenediamine and 0.6 wt% H_2O_2. The research group of Babu et al. found that, when polished with the slurry containing 0.13 M ethylenediamine and 5 wt% H_2O_2, the dissolution rate and polishing rate of copper increased as pH increased, indicating that $–NH_2$ functional groups are more active to bind cooper ions in alkaline environment [16, 17]. In short, pH plays an important role in the polishing performance of $–NH_2$ functional groups of complexing agents. However, the investigation of the effect of $–NH_2$ functional groups of complexing agents on the CMP of GCr15 steel, a typical bearing steel, is still lacking. In our previous work, it was found that the organic base, highly likely a type of amine, in TiSol-NH_4 dispersion could serve as a complex agent to achieve efficient CMP of GCr15 steel [18]. Moreover, our preliminary experimental results reveal that, the MRR of GCr15 steel gradually decreases rather than increases when it is polished with TiSol-NH_4 dispersion and pH value increases from 5.0 to 7.0, which is apparently different from that of copper [16, 17]. Therefore, it is significant to figure out the role of $–NH_2$ functional groups of complexing agents in GCr15 steel CMP.

In this study, ethylenediamine ($H_2NCH_2CH_2NH_2$) with merely two $–NH_2$ functional groups was used as the complexing agent [16, 17] for GCr15 steel CMP to exclude the interference from other functional groups such as –COOH functional groups. In most cases, a proper oxidizer is essential to obtain a high metal MRR by the synergistic effect of oxidation and complexation since complexing agents cannot directly dissolve metal. Conventionally, H_2O_2 has been used as a strong oxidizer for metals CMP since it is readily available and free of contamination [19]. It was found that, when GCr15 steel was polished with the slurries containing H_2O_2 and glycine, with the increase in the H_2O_2 content, the MRR of GCr15 steel reached the peak value at 0.01 wt% H_2O_2 and nearly the valley value at 0.1 wt% H_2O_2, indicating that 0.01 wt% and 0.1 wt% H_2O_2 can provide two typical chemical-mechanical states, respectively [13]. In light of these, 0.01 wt% and 0.1 wt% H_2O_2 as the proper oxidation conditions together with ethylenediamine were used to elucidate the role of $–NH_2$ functional groups of complexing agents for GCr15 steel CMP. The effect of $–NH_2$ functional groups of ethylenediamine on the polishing performance of GCr15 steel was studied as a function of pH value. The corresponding surface film of GCr15 steel was characterized by various experiments including static etching, electrochemical and atomic force microscopy (AFM) wear experiments as well as X-ray photoelectron spectroscopy (XPS) measurements. Afterward, a preliminary polishing mechanism of GCr15 steel was put forward. Additionally, the effect of $–NH_2$ functional groups of ethylenediamine was further assessed on other iron-based metals, including pure iron and a medium carbon 45 steel (also named AISI 1045 steel).

2 Material and methods

Polishing slurries were prepared with deionized (DI) water, colloidal silica (YZ8040 with an average particle size of approximately 80 nm, purchased

from Shanghai YZ-Lapping Material Co., Ltd.), and chemical reagents including ethylenediamine sulfate (purchased from TCI (Shanghai) Development Co., Ltd.) and H_2O_2 (purchased from Sinopharm Chemical Reagent Co., Ltd.). After all the components were added and mixed homogenously, the pH was adjusted with dilute H_2SO_4 and KOH. In this study, ethylenediamine sulfate was used to provide ethylenediamine since ethylenediamine has an ultra-strong alkalinity. The ultra-strong alkalinity will bring about several issues, such as dissolution of colloidal silica [20], and the addition of a large quantity of H_2SO_4 for adjusting pH to neutral and acidic range.

Polishing experiments were performed on a benchtop polisher (UNIPOL-1200S, Shengyang Kejing Auto-instrument Co., Ltd, China). A GCr15 steel disk with diameter of 50.8 mm and thickness of 1.5 mm was polished under the following polishing conditions: set-pressure of 5.0 kg, carrier speed/platen speed of 60 rpm/60 rpm, slurry flow rate of and polishing time of 1 min. The polishing pad used in the experiments was an IC1010/Suba-IV composite pad with K-type groove. In between each polishing step, a pad *ex-situ* conditioning was carried out with a diamond conditioning disk. Before the polishing, the disk was pre-polished to obtain a surface roughness R_a of approximately 2.7 nm. After polishing, the MRR was calculated by measuring the weight loss with a Sartorius ME36S microbalance (1 μg readability). The post-CMP surface morphology was measured by using an optical 3D surface profiler (Chotest SuperView W1, Chotest Technology Inc., China), and the surface roughness R_a was calculated with the analysis software coming with the instrument. The corresponding measured surface area was 97.9 μm × 97.9 μm. If no otherwise specified, each experimental condition was repeated at least four times for all the polishing and characterization experiments.

In order to investigate the pure corrosion of GCr15 steel caused by the slurries, static etching experiments were carried out at room temperature. A GCr15 steel disk with diameter of 25.4 mm and thickness of 1.5 mm was first mechanically polished with an abrasive paper made of silicon carbide (P2000), and then was degreased with ethyl alcohol and cleaned with DI water. Afterwards, it was immersed in the designated solution (without adding abrasive) for 3 min, during which the solution was gently stirred to ensure the uniform dispersion. The static etching rate (SER) was calculated by measuring the weight loss. Given the fact that the mechanically polished surface of GCr15 steel is so rough that it is practically impossible to characterize the post-etching surface morphology, a GCr15 steel sample of 7 mm by 7 mm was first pre-polished with the slurry (pH of 10.0) containing 2 wt% colloidal silica, 0.1 M ethylenediamine sulfate, 0.01 wt% H_2O_2, and DI water to obtain a smooth surface with 1.9 nm R_a, and then it was immersed in the designated solution (without adding abrasive) for 1 min. Afterward, the post-etching surface morphology was measured by using the optical 3D surface profiler, and an AFM (SPA-300HV/SPI3800N Probe Station, Seiko, Japan) in much smaller areas of 10 μm × 10 μm and 1 μm × 1 μm with a silicon nitride AFM probe (MSCT, Bruker, USA, nominal radius of curvature less than 20 nm).

In order to characterize the electrochemical properties of GCr15 steel in the designated solutions (without adding abrasive), electrochemical experiments, including open-circuit potential (OCP), electrochemical impedance spectroscopy (EIS) and potentiodynamic polarization, were performed by using an electrochemical workstation (Autolab PGSTAT 302N, Metrohm Autolab B.V., Switzerland) with a 200 mL three-electrode cell. A platinum electrode was employed as the counter electrode, an Ag/AgCl electrode with a saturated KCl reference solution was employed as the reference electrode, and a cylindrical GCr15 steel sample of 5 mm diameter was employed as the working electrode, which was encased in epoxy resin and electrically connected through a copper wire. Prior to each measurement, the working electrode was first mechanically polished with an abrasive paper made of silicon carbide (P2000), and then was degreased with ethyl alcohol and cleaned with DI water. For each experimental condition, the OCP

measurement was first carried out for 30 min to obtain a steady state. Then, the EIS measurement was performed in the frequency range from 100 kHz to 0.1 Hz with a sinusoidal AC perturbation of 5 mV amplitude. The disturbance electrical signal was applied on the basis of the corresponding open-circuit potential. Afterward, the potentiodynamic polarization measurement was conducted with a scan rate of 1 mV/s and a step of 0.45 mV. The EIS data was analyzed by equivalent electrical circuit modeling with the NOVA analysis software.

In order to further assess the corrosion-enhanced wear of GCr15 steel caused by the slurries, wear tests of a pretreated GCr15 steel sample rubbed against a chemically inert cone-shaped diamond tip (NC-LC, Adama, Ireland, spring constant of 94.25 N/m, and nominal radius of curvature of 20 nm) were conducted on an AFM (SPA-300HV/SPI3800N Probe Station, Seiko, Japan) in vacuum. The experimental conditions were set as follows: applied load F_n of 2–10 μN, relative sliding velocity v of 0.5 μm/s, relative sliding length L of 1 μm, and reciprocating sliding cycle N of 1. Prior to each test, a GCr15 steel sample of 7 mm by 7 mm was first pre-polished with the slurry (pH of 10) containing 2 wt% colloidal silica, 0.1 M ethylenediamine sulfate, 0.01 wt% H_2O_2 and DI water, and a smooth surface with 1.9 nm R_a was acquired. Then, it was immersed in the designated solution (without adding abrasive) for 1 min. Afterward, it was rinsed with DI water, dried, and then immediately placed in a vacuum chamber for the wear test. After the wear test, a silicon nitride AFM probe (MSCT, Bruker, USA) was used to scan the surface topography of the wear area in vacuum.

In order to characterize the chemical composition of the post-CMP and post-etching GCr15 steel surfaces, XPS measurements were performed on an X-ray photoelectron spectrometer (AXIS Ultra DLD, Kratos Analytical, United Kingdom) with a hemispherical energy analyzer and 128 channel detectors. Prior to the measurement, the GCr15 steel sample was either pre-polished or pre-etched with the designated slurries (the etching solutions did not contain the abrasive). Afterward, it was rinsed with DI water, dried, and then immediately placed in a vacuum chamber. The XPS vacuum chamber pressure was less than 7×10^{-10} mbar. All the spectra were obtained at 90° photoelectron take-off angle from the surface. The high-resolution spectra of Fe, Cr, O, and N were measured. Afterward, CasaXPS software was employed to analyze the data.

3 Results and discussion

3.1 Effect of –NH_2 functional groups on the polishing performance of GCr15 steel at different pH

The effect of –NH_2 functional groups of ethylenediamine on the polishing performance of GCr15 steel was studied as a function of pH. The corresponding MRR and surface roughness R_a of GCr15 steel are shown in Fig. 1, and the typical post-CMP surface morphologies of GCr15 steel are displayed in Fig. 2. The slurries were composed of 2 wt% colloidal silica, 0.1 M ethylenediamine sulfate, 0.01 wt% or 0.1 wt% H_2O_2, DI water, and with different pH ranging from 2.0 to 10.0. It can be seen from Fig. 1 that, in the presence of 0.01 wt% H_2O_2 and 0.1 M ethylenediamine, the MRR of GCr15 steel gradually decreases from 275 nm/min at pH 2.0 to 205 nm/min at pH of 4.0, and then to 21 nm/min at pH of 10.0. It should be noted that the MRR decreases to approximately one tenth as pH rises from 4.0 to 10.0. The surface

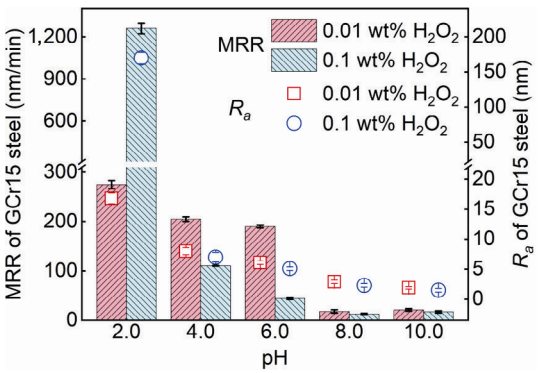

Fig. 1 Effect of –NH_2 functional groups of ethylenediamine on the polishing performance of GCr15 steel as a function of pH. The surface roughness R_a of GCr15 steel under each experimental condition is the average value of those at four different positions on the post-CMP surface.

roughness R_a of GCr15 steel reduces from 16.8 nm at pH of 2.0 to 8.0 nm at pH of 4.0, and then to 1.9 nm at pH of 10.0. It can be clearly observed from Figs. 2(a) and 2(f) that, a large number of corrosion pits are formed on the post-CMP surface of GCr15 steel at pH of 2.0. With pH increasing, the number of corrosion pits gradually decreases, and the post-CMP surface becomes more compact and smoother.

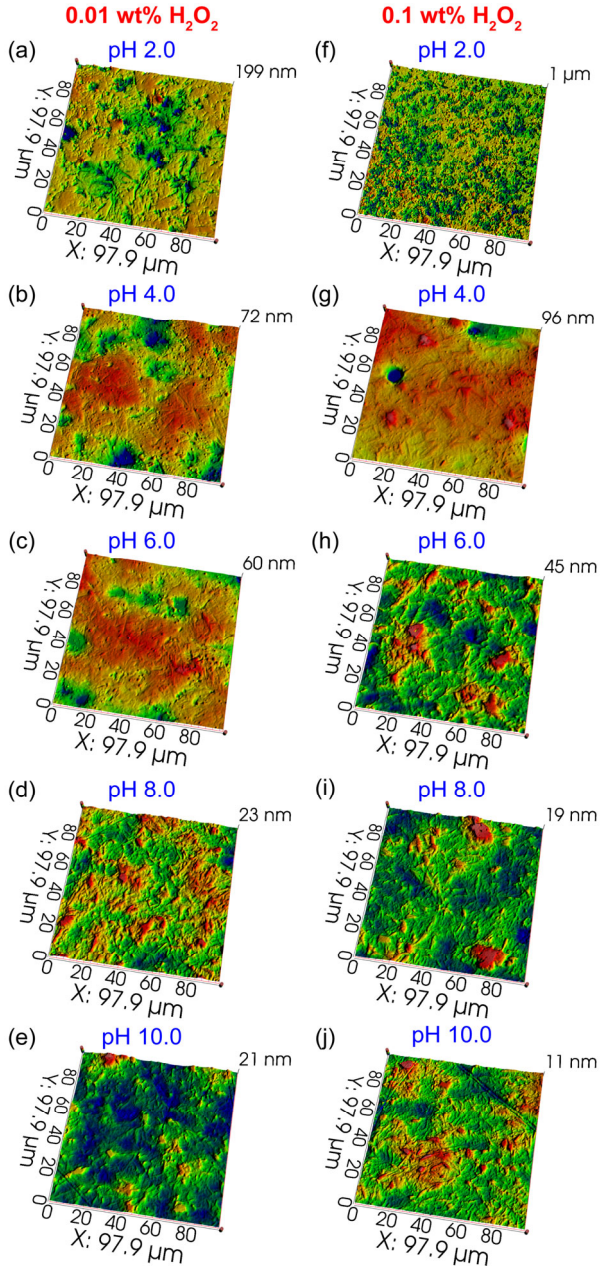

Fig. 2 Typical post-CMP surface morphologies of GCr15 steel after being polished with ethylenediamine and H_2O_2-based slurries at different pH. Under the condition of (a–e) 0.1 M ethylenediamine and 0.01 wt% H_2O_2 and (f–j) 0.1 M ethylenediamine and 0.1 wt% H_2O_2.

Similarly, in the presence of 0.1 wt% H_2O_2 and 0.1 M ethylenediamine, the MRR of GCr15 steel first dramatically decreases from 1,260 nm/min at pH of 2.0 to 110 nm/min at pH of 4.0, and then gradually decreases to 17 nm/min at pH of 10.0. The MRR decreases to approximately one sixth as pH rises from 4.0 to 10.0. The surface roughness R_a of GCr15 steel first sharply reduces from 169.7 nm at pH of 2.0 to 7.0 nm at pH of 4.0, and then gradually decreases to 1.5 nm at pH of 10.0.

In addition, at pH of 2.0, 0.1 wt% H_2O_2 leads to a higher MRR of GCr15 steel than 0.01 wt% H_2O_2, which is different from other pH values from 4.0 to 10.0 [13, 21]. As reported, at pH of 2.0, the direct dissolution of copper could be the main reaction, and the influence of $-NH_2$ functional groups of complexing agents could be insignificant [22]. Similarly, for the case of GCr15 steel, the main reaction at pH of 2.0 could be the direct dissolution by H^+ and H_2O_2. Besides, the presence of H_2O_2 could accelerate the dissolution process [23]. As pH increases to 4.0 and even higher, the molar concentration of H^+ decreases to 10^{-4} M and lower, and the influence of H^+ diminishes gradually. In this case, a high concentration of H_2O_2, such as 0.1 wt%, will lead to the rapid formation of oxides on the GCr15 steel surface, which could serve as a passivation film to hinder the mechanical abrasion, and thus 0.1 wt% H_2O_2 leads to a lower MRR of GCr15 steel than 0.01 wt% H_2O_2 [13].

Based on the polishing results, in both of the two distinct chemical-mechanical states with the addition of either 0.01 wt% or 0.1 wt% H_2O_2 and 0.1 M ethylenediamine, the MRR and surface roughness R_a of GCr15 steel gradually decrease when pH increases, indicating pH has a significant impact on the performance of $-NH_2$ functional groups of ethylenediamine for GCr15 steel CMP. Moreover, it should be pointed out particularly that, the MRR trend of GCr15 steel as pH changes is entirely different from that of copper as reported, where the copper MRR gradually increased as pH increased with ethylenediamine as the complexing agent [16, 17].

3.2 Characterization of the surface film of GCr15 steel formed by –NH_2 functional groups at different pH

As shown in Fig. 1, the MRR and surface roughness R_a of GCr15 steel obtained at pH of 4.0 are in sharp contrast to those at pH of 10.0. Therefore, pH of 4.0 and pH of 10.0 along with 0.01 wt% H_2O_2 are chosen as two typical conditions to further investigate the underlying action mechanism of –NH_2 functional groups of ethylenediamine at different pH. It should be put forward that, by referring to the related literatures [23–25], the following discussion mainly focuses on the chemical and electrochemical reactions of iron since it accounts for approximately 96 wt% of GCr15 steel according to the national standard.

The total MRR in CMP can be decomposed into the following four parts [26–29]: the MRR by the pure wear, the MRR by the corrosion-enhanced wear, the MRR by the pure corrosion, the MRR by the wear-enhanced corrosion. Specifically, the MRR by the corrosion-enhanced wear is mainly attributed to the modification of the mechanical strength of the surface film by slurries, especially by the complexing agent [29–31]. In this study, the pure corrosion and the corrosion-enhanced wear caused by –NH_2 functional groups of ethylenediamine were emphatically investigated by using static etching, electrochemical and AFM wear experiments collectively.

The results of the static etching experiments of GCr15 steel are shown in Fig. 3. The etching solutions were composed of 0.1 M ethylenediamine sulfate, 0.01 wt% H_2O_2, DI water, and with pH of 4.0 or pH of 10.0. It can be seen from Fig. 3(a) that, the SER of GCr15 steel at pH of 4.0 is 23.1 nm/min, and in striking contrast, the SER at pH of 10.0 is nearly undetectable. As shown in Fig. 3(b) and 3(c), after being statically etched at pH of 4.0, the surface of GCr15 steel becomes quite porous and rough; In contrast, after being statically etched at pH of 10.0, the surface remains compact and smooth. As shown in Fig. 3(d), the corresponding surface roughness R_a of GCr15 steel with 97.9 μm × 97.9 μm, 10 μm × 10 μm, and 1 μm × 1 μm measured surface areas all substantially confirms the improvement of the post-etching surface quality as pH rises from 4.0 to 10.0.

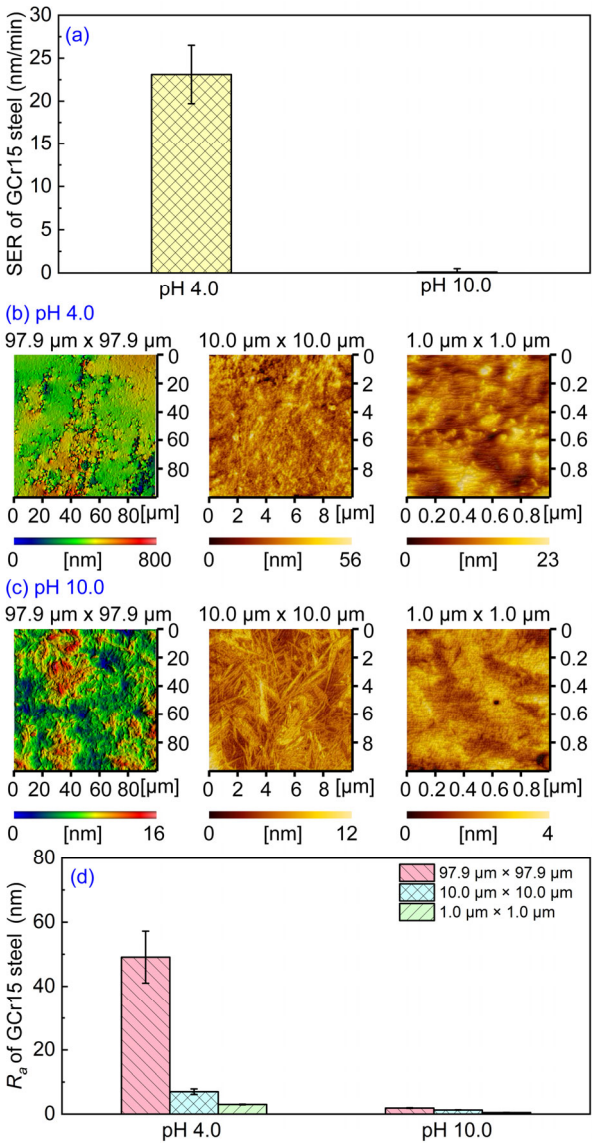

Fig. 3 Results of the static etching experiments of GCr15 steel in the designated ethylenediamine and H_2O_2-based solutions. (a) SER of GCr15 steel; (b, c) typical post-etching surface morphologies of GCr15 steel at pH of 4.0 and pH of 10.0, respectively; and (d) post-etching surface roughness R_a of GCr15 steel.

The results of the electrochemical experiments of GCr15 steel, including OCP and potentiodynamic polarization plots, are shown in Fig. 4. The solutions were composed of 25 mM Na_2SO_4, 0.1 M ethylenediamine sulfate, 0.01 wt% H_2O_2, DI water, and with pH of 4.0 or pH of 10.0. As shown in Fig. 4(a), after 30-min immersion, both of the two

OCP plots at pH of 4.0 and pH of 10.0 become extremely stable, which provides a favorable surface condition for the following electrochemical measurements. Moreover, the OCP value at pH of 4.0 is higher than that at pH of 10.0. The difference in the OCP value should be associated with the change in the anodic and cathodic reactions at different pH [32]. As shown in Fig. 4(b), in comparison with the potentiodynamic polarization plot at pH of 4.0, both the anodic and cathodic reactions of the plot at pH of 10.0 are suppressed pronouncedly, especially the anodic reactions, which is consistent with the trend of the SER results shown in Fig. 3(a). Moreover, at pH of 10.0, an apparent passivation region emerges at an overpotential of approximately –0.4 V (vs. $E_{Ag/AgCl}$) in the anodic curve.

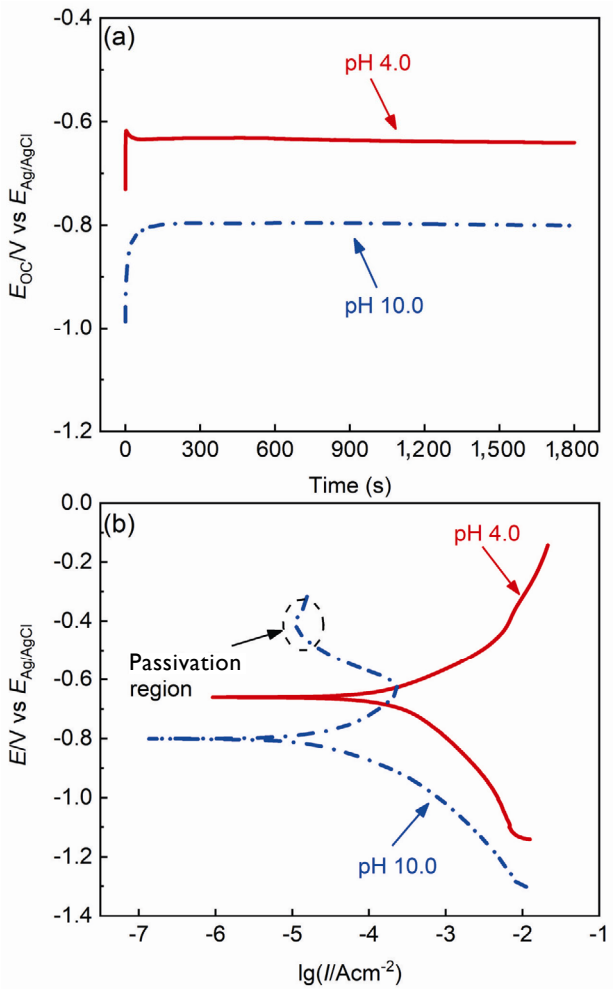

Fig. 4 Results of the electrochemical experiments of GCr15 steel in the designated ethylenediamine and H_2O_2-based electrolytes. (a) OCP plots of GCr15 steel and (b) potentiodynamic polarization plots of GCr15 steel.

More specifically, at pH of 4.0 and with a low concentration of H_2O_2 (0.01 wt%), the main anodic reaction can be depicted as follows [33]:

$$Fe \rightarrow Fe^{2+} + 2e^- \quad (1)$$

The cathodic reaction can be depicted as follows [29]:

$$H_2O_2 + 2H^+ + 2e^- \rightarrow 2H_2O \quad (2)$$

Then, a majority of the reaction product Fe^{2+} are complexed by $-NH_2$ functional groups of ethylenediamine. Specifically, for the acidic form of ethylenediamine, pK_{a1} is 6.85 and pK_{a2} is 9.93 [17, 34]. According to the distribution fraction formula [35], the fractions of the three different species of ethylenediamine, i.e. H_2En^{2+}, HEn^+ and En, in aqueous solution as a function of pH can be calculated, and shown in Fig. 5. Here, En represents $H_2N–CH_2–CH_2–NH_2$.

As shown in Fig. 5, the predominant species of ethylenediamine at pH of 4.0 is H_2En^{2+}. The generated Fe^{2+} are complexed by H_2En^{2+} through forming coordinate bonds involving sharing of the unpaired electrons of nitrogen atoms with empty *d*-orbitals of iron atoms [34, 36]. The complexing reactions can be depicted as follows [37]:

$$[Fe(H_2O)_6]^{2+} + H_2En^{2+} \rightarrow [Fe(H_2O)_4(En)]^{2+} + 2H_3O^+ \quad (3)$$

$$[Fe(H_2O)_4(En)]^{2+} + H_2En^{2+} \rightarrow [Fe(H_2O)_2(En)_2]^{2+} + 2H_3O^+ \quad (4)$$

$$[Fe(H_2O)_2(En)_2]^{2+} + H_2En^{2+} \rightarrow [Fe(En)_3]^{2+} + 2H_3O^+ \quad (5)$$

As a result, soluble $[Fe(H_2O)_m(En)_n]^{2+}$ (where $m+2n=6$) complex compounds are formed [34, 38]

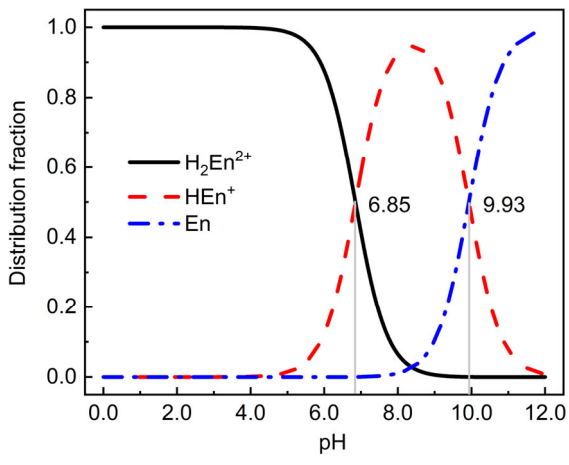

Fig. 5 Calculated distribution diagram showing the fractions of the species of ethylenediamine in aqueous solution as a function of pH according to the distribution fraction formula. En represents $H_2N–CH_2–CH_2–NH_2$.

and dissolved, and then the fresh surface of the GCr15 steel working electrode underneath is exposed continuously, further promoting the anodic and cathodic reactions.

While at pH of 10.0, the anodic reaction is the same as that at pH of 4.0 shown in Eq. (1). The cathodic reactions can be depicted as follows [39]:

$$2H_2O_2 + 2e^- \rightarrow 2OH^- \quad (6)$$

$$O_2 + 2H_2O + 4e^- \rightarrow 4OH^- \quad (7)$$

However, unlike the scenario at pH of 4.0, at pH of 10.0, the reaction product Fe^{2+} can then react with OH^- in the solution as the following reactions [33]:

$$Fe^{2+} + 2OH^- \rightarrow Fe(OH)_2 \quad (8)$$

$$4Fe(OH)_2 + O_2 + 2H_2O \rightarrow 4Fe(OH)_3 \quad (9)$$

$$Fe(OH)_3 \rightarrow FeOOH + H_2O \quad (10)$$

where O_2 in Eqs. (7) and (9) could be either from the dissolved oxygen in the solution or from the decomposition product of H_2O_2 [40]. The oxidation function of O_2 in Eq. (9) can also be achieved by H_2O_2. As a result, insoluble iron hydroxides/oxyhydroxides, such as $Fe(OH)_3$ and FeOOH, can be formed on the GCr15 steel electrode surface, which should primarily account for the suppression of the anodic dissolution. Additionally, as revealed by the following XPS results, ethylenediamine molecules can be adsorbed onto the oxide film as a supplementary protection layer, resulting in the further enhancement of the corrosion resistance [34, 41].

EIS experiments were further carried out to quantitatively investigate the electrochemical properties of the surface film of GCr15 steel formed by $-NH_2$ functional groups of ethylenediamine at different pH. The Nyquist plots and the corresponding equivalent electrical circuits are shown in Fig. 6. The corresponding quantitative fitting results are listed in Table 1. There is merely one semicircle for both pH of 4.0 and pH of 10.0. In the equivalent electrical circuits, R_{sol} represents the solution resistance, R_{ct} represents the charge transfer resistance between the surface film of GCr15 steel and the solution, and CPE_{dl} represents the double layer capacitance between the surface film of GCr15 steel and the solution. According to the fitting results shown in Table 1, when pH changes from 4.0 to 10.0, R_{ct} rises from 77.8 to 921.2 Ω·cm², indicating that the surface film gradually provides effective protection for the substrate of GCr15 steel by restricting the mass transfer of reactants and products between GCr15 steel and the electrolyte [42]. Meanwhile, the admittance Y_{0dl} of CPE_{dl} decreases as pH increases, which could be caused by the increase in the thickness of the electrical double layer [43, 44]. In addition, at pH of 10.0, there is an extra Warburg impedance W associated with the diffusion process of oxygen through the solution to the surface film of GCr15 steel [45]. The above results of the static etching and electrochemical experiments substantially demonstrate that, in the presence of ethylenediamine and H_2O_2, the surface film of GCr15 steel formed at pH of 10.0 can provide a much higher resistance to the pure corrosion than that at pH of 4.0.

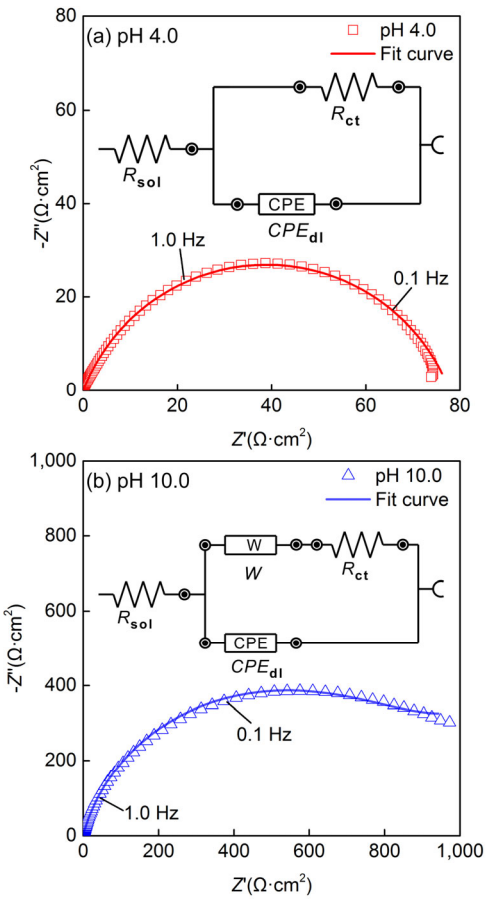

Fig. 6 Nyquist plots and the corresponding equivalent electrical circuits of GCr15 steel in the designated ethylenediamine and H_2O_2-based electrolytes at pH of (a) 4.0 and (b) 10.0.

Table 1 Corresponding quantitative fitting results of Fig. 6.

Solution	R_{sol} ($\Omega\cdot cm^2$)	R_{ct} ($\Omega\cdot cm^2$)	Y_{0dl} ($\mu\Omega^{-1}\cdot cm^{-2}\cdot S^n$)	n	Y_{0W} ($m\Omega^{-1}\cdot cm^{-2}\cdot S^{1/2}$)
pH 4.0	11.4	77.8	989.8	0.769	—
pH 10.0	7.4	921.2	281.1	0.835	5.2

Then, the corrosion-enhanced wear caused by $-NH_2$ functional groups of ethylenediamine was assessed by using AFM wear tests, where the surface film of GCr15 steel was rubbed against a chemically inert diamond tip in vacuum [46]. The immersion solutions for the GCr15 steel pretreatment were composed of 0.1 M ethylenediamine sulfate, 0.01 wt% H_2O_2, DI water, and with pH of 4.0 or pH 10.0. The typical AFM surface topographical images and average cross-section profiles of the wear traces after the wear tests are shown in Figs. 7(a) and 7(b). As displayed in Fig. 7(a), after being pretreated at pH of 4.0, wide and deep wear scars are formed on the GCr15 steel surface by scratching with the diamond tip for one reciprocating sliding cycle; In comparison, after being pretreated at pH of 10.0, narrow and shallow wear scars along with plenty of pileups are formed on the GCr15 steel surface. The width difference in the wear scars could be related to the surface structure. In particular, as shown in Fig. 3(b), at pH of 4.0, the surface of GCr15 steel is porous and rough, and thus the mechanical strength is relatively low. The diamond tip penetrates deeply into the surface and push the material surrounding the tip readily as it scratches, and thereby the wear scar is wide. As show in Fig. 3(c), at pH of 10.0, the surface of GCr15 steel becomes compact and smooth, and thus the mechanical strength grows high. It becomes difficult for the diamond tip to push the surrounding material, and thereby the wear scar is narrow. The corresponding statistical data of the wear depth and volume are shown in Fig. 7(c) and 7(d), respectively. It can be seen that, with the increase in the applied load, both the wear depth and volume almost linearly increase, which could be explained by Archard model [47]. Moreover, both the wear depth and volume at pH of 4.0 are much higher than those at pH of 10.0, suggesting that the surface film of GCr15 steel formed at pH of 10.0 can provide a much higher resistance to the

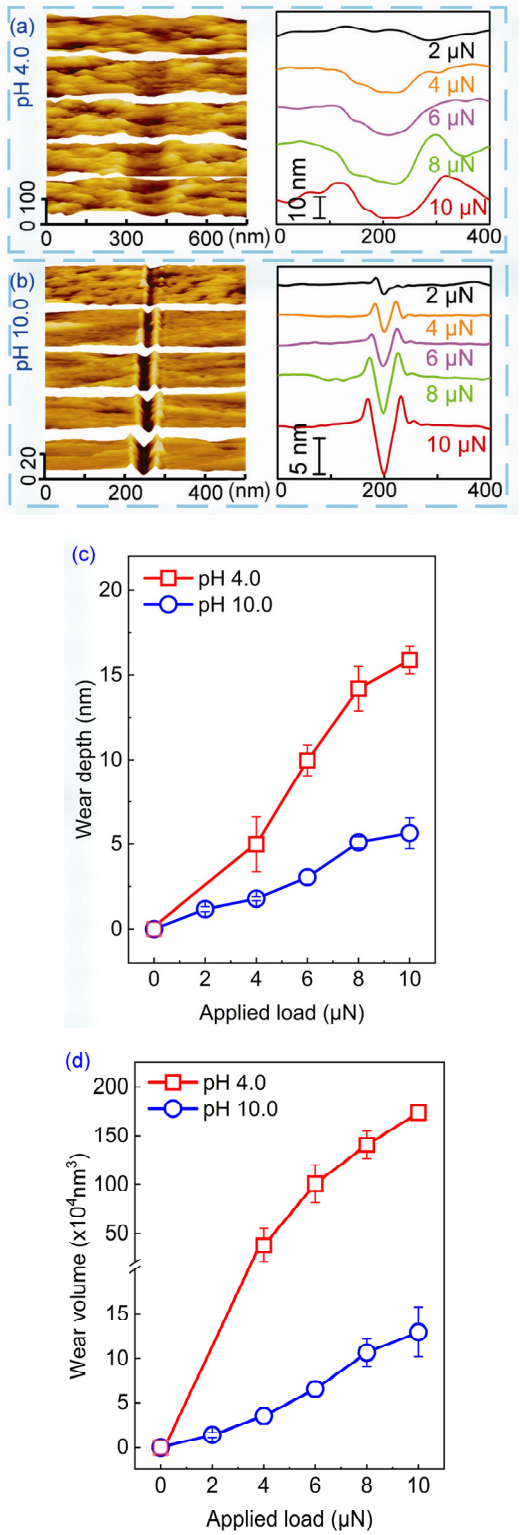

Fig. 7 Results of the AFM wear tests of GCr15 steel after being pretreated with the designated ethylenediamine and H_2O_2-based solutions. (a, b) Typical AFM surface topographical images and average cross-section profiles of the wear traces after the wear tests and (c, d) corresponding statistical data of the wear depth and wear volume.

corrosion-enhanced wear than that at pH of 4.0.

XPS technique was used to further identify the chemical composition of the surface film of GCr15 steel. The XPS spectra of the GCr15 steel surfaces after being either polished or etched are shown in Fig. 8. The polishing slurries were composed of 2 wt% colloidal silica, 0.1 M ethylenediamine sulfate, 0.01 wt% H_2O_2, DI water, and with pH of 4.0 or pH of 10.0. The etching solutions were the same as the polishing slurries except for removing the abrasive. As shown in Fig. 8(a), the deconvolution of Fe($2p_{3/2}$) spectra of both pH of 4.0 and pH of 10.0 reveals three peaks. The left peak with 706.5 eV binding energy should be assigned to metallic Fe [48], the medium peak with 709.6 or 709.3 eV binding energy should be assigned to Fe^{2+} compounds [48, 49], and the right peak with 711.1 or 711.0 eV should be assigned to Fe^{3+} compounds [50, 51]. Moreover, for the polishing preparation method, when pH increases from 4.0 to 10.0, the proportion of metallic Fe keeps approximately 26.0 at%, the proportion of Fe^{2+} compounds decreases from 48.5 at% to 41.0 at%, and the proportion of Fe^{3+} compounds increases from 24.2 at% to 33.3 at%. The etching preparation method shares a similar trend of the proportion change to the polishing one. In combination with the results of static etching and electrochemical experiments, it can be concluded that a more protective layer with a higher Fe^{3+} content can be formed at a higher pH value. As shown in Fig. 8(c), the deconvolution of O(1s) spectra of both pH of 4.0 and pH of 10.0 reveals two peaks, of which that with the lower binding energy at 529.6 eV should be assigned to oxygen as a form of O^{2-} [52], and that with the higher binding energy at 531.3 or 531.1 eV should be assigned to oxygen as a form of OH^- [53]. As shown in Fig. 8(d), the deconvolution of N(1s) spectra of both pH of 4.0 and pH of 10.0 reveals one peak, which should be assigned to nitrogen

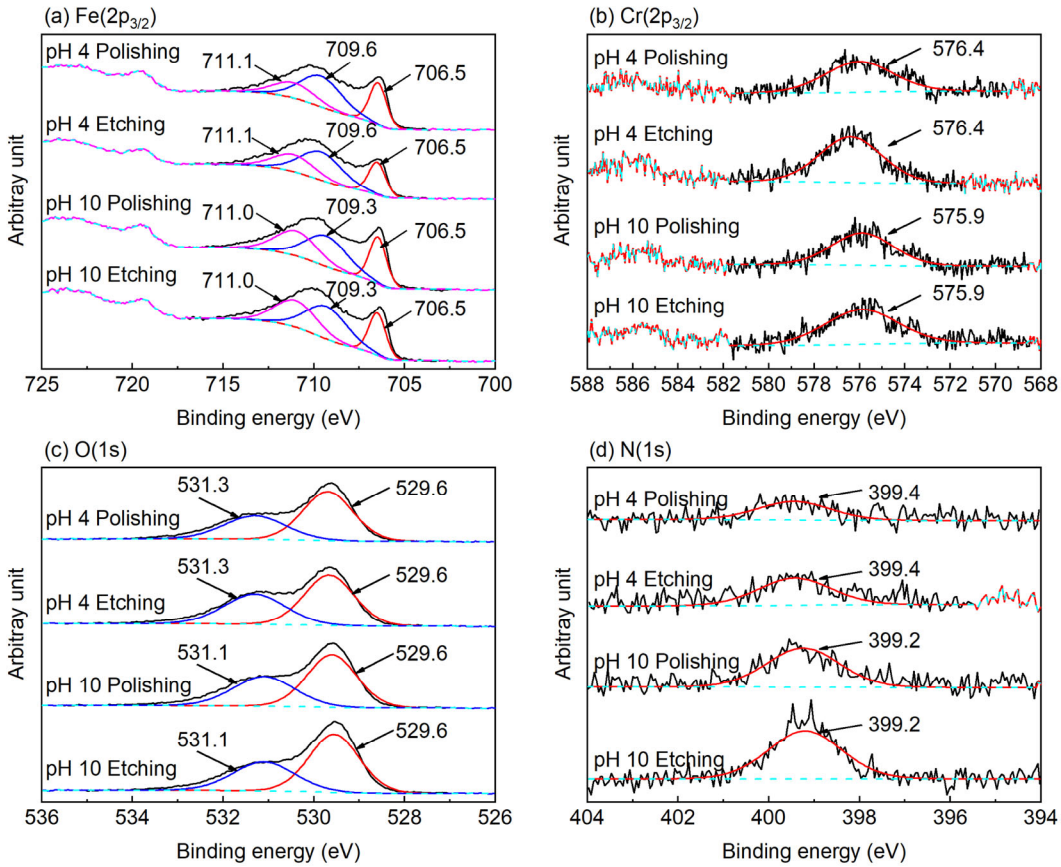

Fig. 8 XPS spectra of the GCr15 steel surfaces after being polished and etched with the designated ethylenediamine and H_2O_2-based slurries (solutions). (a) Fe($2p_{3/2}$); (b) Cr($2p_{3/2}$); (c) O(1s); and (d) N(1s).

atoms of the complex compounds formed by the complexing reactions between iron ions and of $-NH_2$ functional groups of ethylenediamine [36]. Moreover, after being either polished or etched, the area of the N(1s) peak increases when pH changes from 4.0 to 10.0, indicating more ethylenediamine molecules are adsorbed onto the GCr15 steel surface probably due to the complexing reaction between ethylenediamine and Fe^{3+} [41].

3.3 Polishing mechanism of GCr15 steel by $-NH_2$ functional groups at different pH

Summarizing up all the above polishing and characterization results, a preliminary polishing mechanism of GCr15 steel by $-NH_2$ functional groups of ethylenediamine at different pH value can be proposed as follows, and a schematic diagram of the polishing mechanism is depicted in Fig. 9. As shown in Fig. 9(a), in the presence of ethylenediamine and a low concentration of H_2O_2 (0.01 wt%) and at acidic pH of 4.0, Fe^{2+} ions are continuously produced by the oxidation reactions (Eq. (1)), and a majority of Fe^{2+} ions are then complexed by $-NH_2$ functional groups of ethylenediamine to form soluble $[Fe(H_2O)_m(En)_n]^{2+}$ complex compounds (Eqs. (3)–(5)), and severe corrosion occurs on the surface, resulting in a high SER and the formation of a porous and nonuniform surface film with many deep corrosion pits (Fig. 3), which is of a low wear resistance to the mechanical abrasion (Fig. 7). Hence, under such corrosion condition, the MRR and surface roughness R_a is high (Fig. 1); As pH gradually increases to alkaline pH of 10.0, as shown in Fig. 9(b), insoluble Fe^{3+} hydroxides/oxyhydroxides are mainly formed (Eqs. (8)–(10)) on the GCr15 steel surface, then $-NH_2$ functional groups of ethylenediamine are absorbed onto the oxide film to further enhance the corrosion resistance (confirmed by the XPS results shown in Fig. 8), resulting in an extremely low SER and a compact and protective surface film (Fig. 3), which is of a high wear resistance to the mechanical abrasion (Fig. 7). Hence, under such increasingly protective condition, the MRR and surface roughness R_a decrease accordingly.

3.4 Extension to other iron-based metals

To further examine the effect of $-NH_2$ functional groups of ethylenediamine on the polishing performance of other iron-based metals, pure iron and 45 steel were polished with ethylenediamine and H_2O_2-base slurries. The polishing results are shown and compared with those of GCr15 steel in Fig. 10. The slurries were composed of 2 wt% colloidal silica, 0.1 M ethylenediamine sulfate, 0.01 wt% or 0.1 wt% H_2O_2, DI water, and with pH of 4.0 or pH of 10.0. It can be distinctly seen that, in the presence of 0.1 M ethylenediamine and either 0.01 wt% or 0.1 wt% H_2O_2, the three types of iron-based metals share the same trend of the MRR

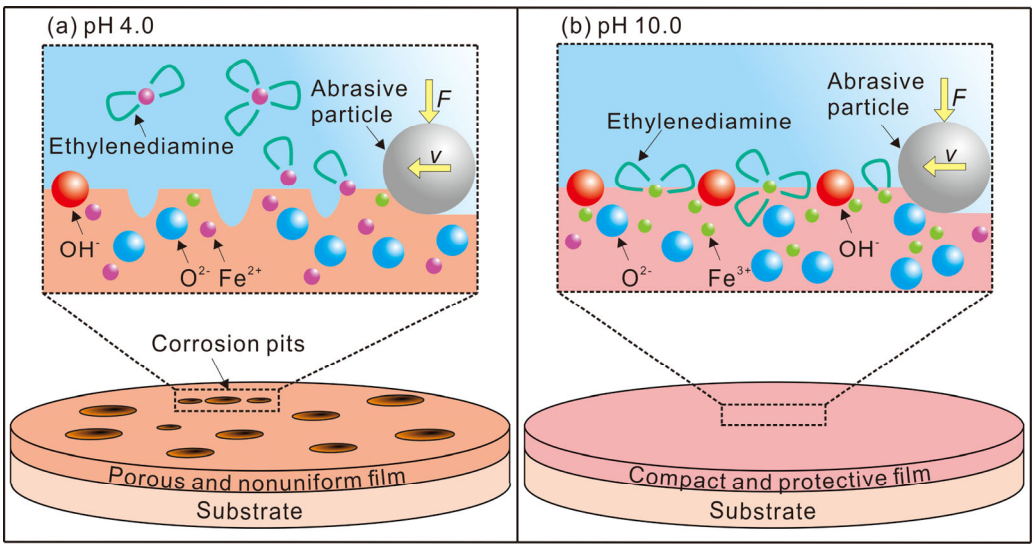

Fig. 9 Schematic diagram of the preliminary polishing mechanism of GCr15 steel.

and surface roughness R_a. Specifically, the MRR and surface roughness R_a both decrease when pH changes from 4.0 to 10.0. Therefore, it can be concluded that the CMP performance of $-NH_2$ functional groups of ethylenediamine at different pH can be potentially applied to other iron-based steels, such as die steel and tool steel.

In summary, the findings of the study provide beneficial guide for screening appropriate amine groups-based complexing agents for CMP of iron-based metals in acidic pH range. More complexing agents, such as polyamines [54], can be evaluated to achieve a high MRR in an acidic environment. Such a high MRR can be used for the initial step of the finishing process of rough surfaces of iron-based metals. More investigation on introducing appropriate corrosion inhibitors as counterparts of complexing agents is needed to balance the corrosion and the protection, so as to achieve a high MRR and a satisfactory surface quality simultaneously.

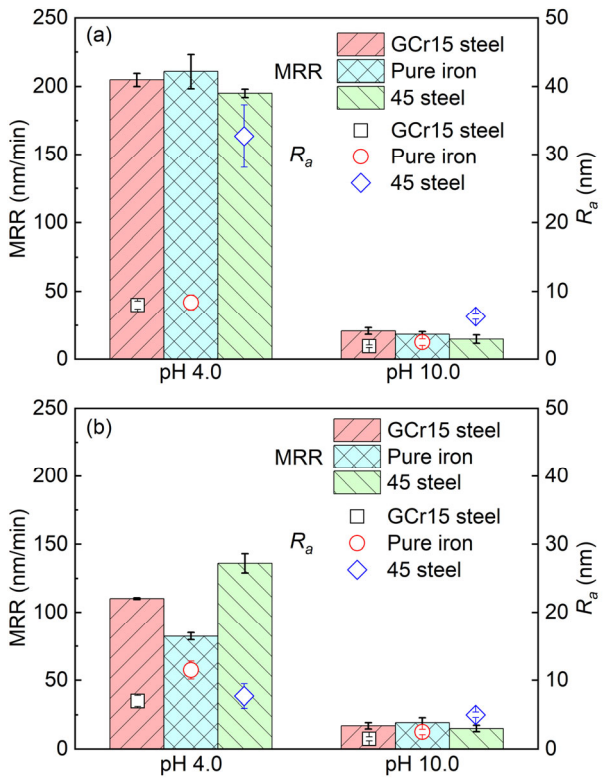

Fig. 10 Effect of $-NH_2$ functional groups of ethylenediamine on the polishing performance of iron-based metals at pH of 4.0 and 10.0 under the condition of (a) 0.1 M ethylenediamine and 0.01 wt% H_2O_2 and (b) 0.1 M ethylenediamine and 0.1 wt% H_2O_2.

4 Conclusions

Ethylenediamine (obtained from ethylenediamine sulfate to avoid the strong alkalinity) with two $-NH_2$ functional groups was introduced into H_2O_2-based slurries as a key complexing agent for GCr15 steel CMP. The role of $-NH_2$ functional groups of ethylenediamine in GCr15 steel CMP and the underlying polishing mechanism were investigated. Additionally, the effect of $-NH_2$ functional groups of ethylenediamine on CMP of other iron-based metals was assessed. Based on the above results and discussion, the conclusions can be reached as follows:

1) In the presence of 0.1 M ethylenediamine and either 0.01 wt% or 0.1 wt% H_2O_2, the MRR and surface roughness R_a of GCr15 steel gradually decrease as pH increases from 2.0 to 10.0, which clearly shows that pH has an effective influence on the polishing performance of $-NH_2$ functional groups of ethylenediamine for GCr15 steel CMP.

2) At pH of 4.0, with the addition of ethylenediamine and a low concentration of H_2O_2, severe corrosion occurs on the surface, which is attributed to the complexation reactions between $-NH_2$ functional groups of ethylenediamine and Fe^{2+} ions to form soluble $[Fe(H_2O)_m(En)_n]^{2+}$ complex compounds, and a porous and nonuniform surface film with a low wear resistance to the mechanical abrasion is formed, and thus the MRR and R_a of GCr15 steel is high. When pH increases to 10.0, a compact and protective surface film with a high wear resistance to the mechanical abrasion, comprising more Fe^{3+} hydroxides/oxyhydroxides and complex compounds with $-NH_2$ functional groups of ethylenediamine, is formed, and thus the MRR and R_a of GCr15 steel decreases.

3) In ethylenediamine and H_2O_2-based slurries, the MRR and surface roughness R_a of the three types of iron-based metals, i.e. GCr15 steel, pure iron and 45 steel, perform the same trend when pH changes from 4.0 to 10.0.

Acknowledgements

The authors are grateful for the financial supports by National Natural Science Foundation of China (51975488, 51991373, and 51605396), National Key R&D Program of China (2018YFB2000400), Science Challenge Project (TZ2018006), Tribology Science Fund of State Key Laboratory of Tribology (SKLTKF16A02), and Laboratory of Precision Manufacturing Technology CAEP (ZD17005).

References

[1] Yin F, Hua L, Mao H, Han X. Constitutive modeling for flow behavior of GCr15 steel under hot compression experiments. *Mater Design* **43**: 393–401 (2013)

[2] Bhadeshia H K D H. Steels for bearings. *Prog Mater Sci* **57**(2): 268–435 (2012)

[3] Mohd Yusof N F, Ripin Z M. Analysis of surface parameters and vibration of roller bearing. *Tribol T* **57**(4): 715–729 (2014)

[4] Takabi J, Khonsari M M. On the dynamic performance of roller bearings operating under low rotational speeds with consideration of surface roughness. *Tribol Int* **86**: 62–71 (2015)

[5] Komata H, Iwanaga Y, Ueda T, Ueda K, Mitamura N. Enhanced performance of rolling bearings by improving the resistance of rolling elements to surface degradation. In *Bearing Steel Technologies: 10th Volume, Advances in Steel Technologies for Rolling Bearings*. Beswick J M, Edn. West Conshohocken, PA: ASTM International, 2015: 272–290.

[6] Chi X, Suo X H. Study on float polishing of metal nanometer surface. *Advanced Materials Research* **154**–**155**: 1757–1760 (2011)

[7] Li Y. *Microelectronic Applications of Chemical Mechanical Planarization*. Hoboken, New Jersey (USA): John Wiley & Sons, Inc., 2007.

[8] Zhao D, Lu X. Chemical mechanical polishing: Theory and experiment. *Friction* **1**(4): 306–326 (2013)

[9] Manabu T. The way to zeros: The future of semiconductor device and chemical mechanical polishing technologies. *Jpn J Appl Phys* **55**(6S3): 06JA01 (2016)

[10] Kao M J, Hsu F C, Peng D X. Synthesis and characterization of SiO_2 nanoparticles and their efficacy in chemical mechanical polishing steel substrate. *Adv Mater Sci Eng* **2014**: 1–8 (2014)

[11] Peng D-X. Chemical mechanical polishing of steel substrate using aluminum nanoparticles abrasive slurry. *Ind Lubr Tribol* **66**(1): 124–130 (2014)

[12] Peng D-X. Optimization of chemical mechanical polishing parameters on surface roughness of steel substrate with aluminum nanoparticles via Taguchi approach. *Ind Lubr Tribol* **66**(6): 685–690 (2014)

[13] Jiang L, He Y, Luo J. Chemical mechanical polishing of steel substrate using colloidal silica-based slurries. *Appl Surf Sci* **330**: 487–495 (2015)

[14] Koroleva L F. Abrasive properties of modified oxides for finish polishing of steel. *AIP Conf Proc* **1915**(1): 040027 (2017)

[15] Liu P, Lu X, Liu Y, Luo J, Pan G. Chemical mechanical planarization of copper using ethylenediamine and hydrogen peroxide based slurry. In *Advanced Tribology*. Luo J, Meng Y, Shao T, Zhao Q, Edns. Springer, Berlin, Heidelberg, 2009: 908–911.

[16] Gorantla V R K, Goia D, Matijević E, Babu S V. Role of amine and carboxyl functional groups of complexing agents in slurries for chemical mechanical polishing of copper. *J Electrochem Soc* **152**(12): G912–G916 (2005)

[17] Patri U B, Aksu S, Babu S V. Role of the functional groups of complexing agents in copper slurries. *J Electrochem Soc* **153**(7): G650–G659 (2006)

[18] Wu H, Jiang L, Liu J, Deng C, Huang H, Qian L. Efficient chemical mechanical polishing of AISI 52100 bearing steel with TiSol-NH_4 dispersion-based slurries.

Tribol Lett **68**(1): 34 (2020)

[19] Hariharaputhiran M, Zhang J, Ramarajan S, Keleher J, Li Y, Babu S. Hydroxyl radical formation in H_2O_2-amino acid mixtures and chemical mechanical polishing of copper. *J Electrochem Soc* **147**(10): 3820–3826 (2000)

[20] Kobayashi M, Juillerat F, Galletto P, Bowen P, Borkovec M. Aggregation and charging of colloidal silica particles: Effect of particle size. *Langmuir* **21**(13): 5761–5769 (2005)

[21] Jiang L, He Y, Yang Y, Luo J. Chemical mechanical polishing of stainless steel as solar cell substrate. *ECS J Solid State Sc* **4**(5): P162–P170 (2015)

[22] Kim Y J, Kwon O J, Kang M C, Kim J J. Effects of the functional groups of complexing agents and Cu oxide formation on Cu dissolution behaviors in Cu CMP process. *J Electrochem Soc* **158**(2): H190–H196 (2011)

[23] Yang C, Zhang H, Guo W, Fu Y. Effects of H2O2 addition on corrosion behavior of high-strength low-alloy steel in seawater. *J Chin Soc Corros Prot* **33**(03): 205–210 (2013)

[24] Wu W, Hao W K, Liu Z Y, Li X G, Du C W, Liao W J. Corrosion behavior of E690 high-strength steel in alternating wet-dry marine environment with different pH values. *J Mater Eng Perform* **24**(12): 4636–4646 (2015)

[25] Wang Z, Liu J, Wu L, Han R, Sun Y. Study of the corrosion behavior of weathering steels in atmospheric environments. *Corros Sci* **67**: 1–10 (2013)

[26] Li J, Liu Y, Lu X, Luo J, Dai Y. Material removal mechanism of copper CMP from a chemical-mechanical synergy perspective. *Tribol Lett* **49**(1): 11–19 (2013)

[27] Li J, Liu Y, Wang T, Lu X, Luo J. Electrochemical investigation of copper passivation kinetics and its application to low-pressure CMP modeling. *Appl Surf Sci* **265**(0): 764–770 (2013)

[28] Tripathi S, Doyle F, Dornfeld D. Tribo-chemical modeling of copper CMP. In *Proceedings of VLSI Multilevel Interconnection Conference (VMIC)*, Fremont CA, 2006: 432–437.

[29] Jiang L, He Y, Li J, Luo J. Passivation kinetics of 1,2,4-Triazole in copper chemical mechanical polishing. *ECS J Solid State Sc* **5**(5): P272–P279 (2016)

[30] Xu G, Liang H, Zhao J, Li Y. Investigation of copper removal mechanisms during CMP. *J Electrochem Soc* **151**(10): G688 (2004)

[31] Ihnfeldt R, Talbot J B. Effect of CMP slurry chemistry on copper nanohardness. *J Electrochem Soc* **155**(6): H412–H420 (2008)

[32] Hiromoto S. 4-corrosion of metallic biomaterials. In *Metals for Biomedical Devices*. Niinomi M, Edn. Woodhead Publishing, 2010: 99–121.

[33] Du C W, Li X G, Liang P, Liu Z Y, Jia G F, Cheng Y F. Effects of microstructure on corrosion of X70 pipe steel in an alkaline soil. *J Mater Eng Perform* **18**(2): 216–220 (2009)

[34] Selwyn L S, Argyropoulos V. Removal of chloride and iron ions from archaeological wrought iron with sodium hydroxide and ethylenediamine solutions. *Stud Conserv* **50**(2): 81–100 (2005)

[35] Wuhan University. *Analytical Chemistry*. Beijing: Higher Education Press, 2016.

[36] Incorvio M J, Contarini S. X. Ray photoelectron spectroscopic studies of metal/inhibitor systems: Structure and bonding at the iron/amine interface. *J Electrochem Soc* **136**(9): 2493–2498 (1989)

[37] Nicholls D. The chemistry of iron, cobalt and nickel. In *Comprehensive Inorganic Chemistry*. JR J C B, Emeléus F R S H J, Sir Ronald Nyholm F R S, Trotman-Dickenson A F, Edns. Oxford: Pergamon Press, 1973.

[38] Sakakibara M, Nishihara H, Aramaki K. The effects of complexing agents on the corrosion of iron in an anhydrous methanol solution. *Corros Sci* **34**(12): 1937–1946 (1993)

[39] Jiang L, He Y, Liang H, Li Y, Luo J. Effect of potassium ions on tantalum chemical mechanical polishing in H_2O_2-based alkaline slurries. *ECS J Solid State Sc* **5**(2): P100–P111 (2016)

[40] Kuiry S C, Seal S, Fei W, Ramsdell J, Desai V H, Li Y, Babu S V, Wood B. Effect of pH and H_2O_2 on Ta Chemical mechanical planarization: Electrochemistry and X-ray photoelectron spectroscopy studies. *J Electrochem Soc* **150**(1): C36–C43 (2003)

[41] Zhang M, Chen K, Chen X, Peng X, Sun X, Xue D. Ethylenediamine-assisted crystallization of Fe_2O_3 microspindles with controllable size and their pseudocapacitance performance. *Cryst Eng Comm* **17**(7): 1521–1525 (2015)

[42] López D A, Simison S N, de Sánchez S R. Inhibitors performance in CO_2 corrosion: EIS studies on the interaction between their molecular structure and steel microstructure. *Corros Sci* **47**(3): 735–755 (2005)

[43] Ashassi-Sorkhabi H, Seifzadeh D, Hosseini M G. EN, EIS and polarization studies to evaluate the inhibition effect of 3H-phenothiazin-3-one, 7-dimethylamin on mild steel corrosion in 1M HCl solution. *Corros Sci* **50**(12): 3363–3370 (2008)

[44] Ashassi-Sorkhabi H, Shaabani B, Seifzadeh D. Effect of some pyrimidinic Shciff bases on the corrosion of mild steel in hydrochloric acid solution. *Electrochim Acta*

50(16): 3446–3452 (2005)
[45] Qiao G, Ou J. Corrosion monitoring of reinforcing steel in cement mortar by EIS and ENA. *Electrochim Acta* **52**(28): 8008–8019 (2007)
[46] Bai M, Kato K, Umehara N, Miyake Y, Xu J, Tokisue H. Scratch–wear resistance of nanoscale super thin carbon nitride overcoat evaluated by AFM with a diamond tip. *Surf Coat Tech* **126**(2): 181–194 (2000)
[47] Archard J F. Contact and rubbing of flat surfaces. *J Appl Phys* **24**(8): 981–988 (1953)
[48] Mills P, Sullivan J L. A study of the core level electrons in iron and its three oxides by means of X-ray photoelectron spectroscopy. *J Phys D: Appl Phys* **16**(5): 723–732 (1983)
[49] Wu H, Huang F, Lu X, Xu T, Lu X, Ti R, Jin Y, Zhu J. Grain size and Fe^{2+} concentration-dependent magnetic, dielectric, and magnetodielectric properties of $Y_3Fe_5O_{12}$ ceramics. *Phys Status Solidi A* **213**(1): 146–153 (2016)
[50] Brienne S H R, Zhang Q, Butler I S, Xu Z, Finch J A. X-ray photoelectron and infrared spectroscopic investigation of sphalerite activation with iron. *Langmuir* **10**(10): 3582–3586 (1994)
[51] Allen G C, Curtis M T, Hooper A J, Tucker P M. X-Ray photoelectron spectroscopy of iron–oxygen systems. *J Chem Soc, Dalton Trans* (14): 1525–1530 (1974)
[52] Stoch J, Gablankowska-Kukucz J. The effect of carbonate contaminations on the XPS O 1s band structure in metal oxides. *Surf Interface Anal* **17**(3): 165–167 (1991)
[53] Horváth D, Toth L, Guczi L. Gold nanoparticles: Effect of treatment on structure and catalytic activity of Au/Fe_2O_3 catalyst prepared by co-precipitation. *Catal Lett* **67**(2): 117–128 (2000)
[54] Jiang L, Lan Y, He Y, Li Y, Luo J. Functions of Trilon® P as a polyamine in copper chemical mechanical polishing. *Appl Surf Sci* **288**: 265–274 (2014)

Hanqiang WU. He received his bachelor degree in mechanical engineering in 2017 from Southwest Jiaotong University, Chengdu, China, and his master degree in mechanical engineering in 2020 from the same university. He is currently a Ph.D. in the Laboratory for Extreme Manufacturing Science at Southern University of Science and Technology. His research interest includes chemical mechanical polishing and ultrasonic assisted plasma oxidation grinding.

Liang JIANG. He is an associate professor in mechanical engineering at Southwest Jiaotong University, Chengdu, China. He received his bachelor degree in mechanical engineering in 2009 from Harbin Institute of Technology, Harbin, China, and his Ph.D. degree in mechanical engineering in 2015 from Tsinghua University, Beijing, China. During the period 2010–2012, he studied as a joint Ph.D. student in Clarkson University, Potsdam, New York, USA. Then he joined the faculty at Southwest Jiaotong University in 2015. His research interest focuses on chemical mechanical polishing.